ELSEVIER

Coordination Chemistry Reviews
200–202 (2000) 411–442

COORDINATION CHEMISTRY REVIEWS

www.elsevier.com/locate/ccr

The application of electrochemical scanning probe microscopy to the interpretation of metalloprotein voltammetry

Jason J. Davis [a], H. Allen O. Hill [a,*], Alan M. Bond [b]

[a] *Inorganic Chemistry Laboratory, University of Oxford, South Parks Road, Oxford OX1 3QR, UK*
[b] *Department of Chemistry, Monash University, Clayton, Victoria, 3168, Australia*

Received 21 September 1999; accepted 23 February 2000

Contents

* Corresponding author. Tel./fax: +44-1865-275900.
E-mail address: allen.hill@chem.ox.ac.uk (H.A.O. Hill).

PII: S0010-8545(00)00321-0

Abstract

An accurate interpretation of metalloprotein voltammetry depends critically on a detailed understanding of the electrode surface and its interactions with surface-active proteins. Representations of the bioelectrochemical interface as a uniformly electroactive, flat electrode surface, where electron transfer takes place to non surface-interacting proteins, are unrealistic. The development of scanning probe technology allows both these surfaces and the interactions of biomolecules to be probed with an unprecedented resolution. In this review, the results of a number of scanning probe studies are presented, together with the theoretical implications for more realistic models required in the interpretation of metalloprotein voltammetric experiments.

Keywords: Scanning probe microscopy; Electrodes; Voltammetry; Protein; Adsorption

1. Introduction

Electron transfer reactions of biomolecules are central to the most fundamental processes of life [1]. Respiration, for example, is the stepwise oxidation of an organic substrate through a series of redox reactions involving a chain of electron acceptors, between which electrons are shuttled by electron carriers such as cytochromes, iron–sulphur proteins and flavin nucleotide coenzymes. These same molecules play a similar role in the photo-induced electron transfer chains of photosynthesis. Consequently, the study of metalloprotein electrochemistry should provide invaluable insights into the dynamic behaviour of the molecules intimately involved in meeting the energy requirements of all living organisms.

The methods of metalloprotein bioelectrochemistry, especially the voltammetric techniques introduced more than 20 years ago [2,3], provide a powerful tool by which the electron transfer properties of these redox proteins can be probed. By studying the kinetics and thermodynamics of the interactions between metalloproteins and electrode surfaces, our understanding of in vivo electron transfer processes has increased considerably. Additionally, voltammetric studies have been of fundamental importance to the development of bioanalytical systems [4].

In the early stages of metalloprotein voltammetric studies, the importance of the electrode surface interactions was recognised. At this time, however, the data obtained from current/potential/time curves were not adequate to define unambiguously these inherently very complex interfacial processes. In recent years it has emerged that the application of scanning probe microscopy (SPM) to the characterisation of electrode surfaces, and the chemical processes which occur at them,

provides an invaluable means of increasing our understanding of these interactions [5,6]. A tool is thus now available to provide guidance for the realistic use of electrochemical models that should be applied to metalloprotein–electrode surface reactions. In this review, the principles and application of SPM to metalloprotein surface interactions and voltammetry (at both gold and carbon electrodes) will be outlined and the impact of this information on the subject of bioelectrochemical electrochemistry will be discussed.

1.1. Interactions of protein with the electrochemical surface

Since the electrode surface (and interactions in the interfacial region) are integral to the expression of protein electrochemistry [7,8], it follows that a detailed knowledge of both the structure and properties of the electrode/protein/electrolyte interface is necessary if the nuances of the electron transfer coupled surface reactions which take place are to be understood. Though surface reactions at electrodes can be probed by methods such as surface-enhanced resonance Raman (SERRS), ellipsometry, and IR spectroscopy, none of these techniques is able to provide direct real-space information on the electrode surface topography nor the molecular-level resolution of species present at the interface. Ideally, it is exactly this level of detail that is required in modelling voltammetry.

The application of scanning probe microscopy to the study of surfaces in three-dimensions has grown enormously since the invention [9] of the scanning tunnelling microscope (STM) in 1982, and the atomic force microscope (AFM) four years later [10]. In particular, recent advances in both software and hardware render these techniques powerful in resolving the surface topography of materials down to an atomic level with seemingly non-destructive probes [11]. Thus it is not surprising that results obtained through the SPM imaging of both macroelectrode (carbon and gold) surfaces and microelectrode arrays, as presented in this review article, provide new knowledge which significantly enhances our understanding of the details of complex electrochemical processes that occur when highly surface-active metalloproteins are reduced or oxidised under voltammetric conditions at such electrodes. Ideally, we suggest that, in future, it should be the results of these direct surface observations (and surface interactions) which provide the basis for the application of rational voltammetric models to describe protein electrochemistry (as an alternative to the somewhat arbitrary and empirical use of postulated models as has been the case in the past).

1.2. Scanning probe microscopy

The generic term, scanning probe microscopes (SPMs), encompasses a wide range of high-resolution surface mapping apparatus. Scanning probe microscopy involves the movement of a probe across a surface to generate an image representative of a specific (according to the probe) property of that surface. The STM was the first instrument capable of generating real-space images of a surface with an atomic-level resolution. Data are taken from the tunnelling current (typically a nanoampere or

less) generated on scanning a very sharp (ideally terminating in a single atom) conductive tip across a conductive sample, held at a fixed potential. The early success of the STM led to the development of the AFM. This method does not require the scanned surface to be conductive and can accordingly be applied to a much wider range of materials. The AFM is a device capable of measuring ultra-small forces; forces on particles as small as atoms. It measures, in effect, contours of force; the tip 'reads' the surface forces much like the stylus of a phonograph 'reads' a record. Forces can be measured by monitoring the elastic deformation of a spring. If this spring is of very low mass, and its deformation can be measured exceedingly accurately, then incredibly small forces can be detected. With AFM, the spring is a cantilever (on the end of which is the probe) and its motion is measured, usually, with a laser beam. The force required to move the cantilever through measurable distances can be as small as 10^{-18} N and it is this level of sensitivity that allows the imaging of forces between single atoms. Almost any material can be imaged through use of a variety of forces (Born repulsion, van der Waals, magnetic, electrostatic, etc.). The demonstration [12] that these scanning processes (both AFM and STM) are not limited to vacuum but can also be carried out in air and under electrolytic solution, represented a very significant advance.

The mechanical basis of an atomic force microscope, applied in the electrochemical studies presented in this review, is then simple; one requires a sharp tip attached to a soft, flexible cantilever spring, a deflection sensing system, a precise movement system and a data analysis/acquisition system (Fig. 1). The set-up for a scanning tunnelling microscope is largely the same with the exception that the current between a sharp metallic tip and the substrate electrode is monitored. For electrochemical studies, a four-electrode system is used, with both tip and substrate potentials referenced to a designated fixed potential.

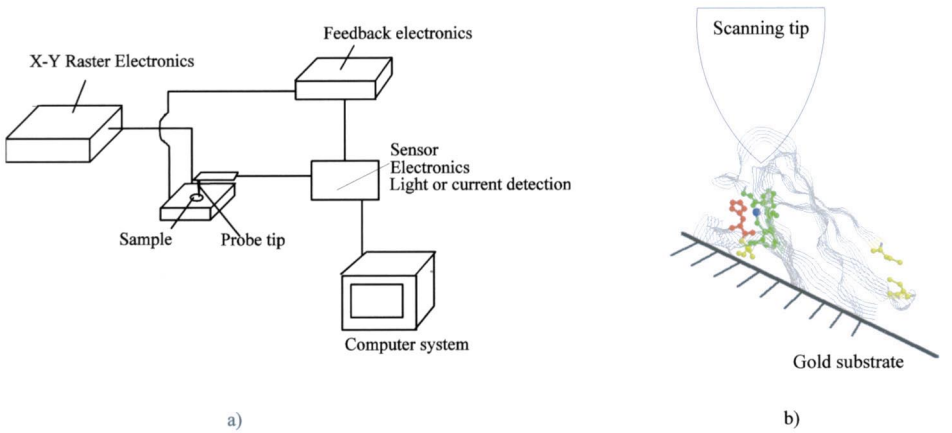

Fig. 1. (a) The basic components of a scanning probe microscope; an x, y piezoelectric scanner, a sensor to monitor movement of the probe, feedback circuits for controlling the z-piezo and a computer system on which results can be displayed and analysed. (b) Proposed azurin S118C tunnelling configuration. Cysteine residues yellow. Binding is assumed to be 'side-on' through cysteine 113.

The movement system (the 'scanner') is a 3D piezoelectric drive. Usually, the sample is attached to this scanner and can be moved, very precisely, beneath the tip in x, y and z directions. Central to the development of these microscopes has been the advance in piezoelectric technology. Piezoelectric elements are ceramic electromechanical transducers that change size ever-so-slightly in response to an electric field; they allow control of motion down to the angstrom level. The scanner is moved very precisely, in a raster motion, with respect to the tip by applying appropriate voltages to the three (x, y, z) rods. The force acting on the cantilever (or the tunnelling current in the case of STM) is kept constant by a feedback loop, and the variant voltage applied by this to the scanner is used in the generation of a 3D force or tunnelling map of the surface (a 'topographic map').

2. SPM characterisation of electrode surfaces relevant to metalloprotein voltammetry

Two electrode surfaces where SPM data can be readily obtained, and where extensive amounts of voltammetric data are available, are gold and pyrolytic graphite.

2.1. SPM characterisation of metalloprotein–gold interactions

2.1.1. Studies at single crystalline Au[111] surfaces

Traditionally, polycrystalline gold has been one of the most commonly used electrode surfaces in metalloprotein electrochemistry. The results of recent SPM studies of metalloprotein interactions with this surface can, therefore, be related to a long history of published voltammetric data. One of the principal requirements for molecular-level scanning probe investigations, is, however, the use of pristine, atomically-flat substrate surfaces. Unfortunately, polycrystalline gold macroelectrodes, used in the majority of bioelectrochemical investigations, are insufficiently flat on a micrometer scale for molecular-level imaging of protein molecules to be feasible (see below). Atomically-flat, single crystalline (Au[111]) evaporated gold films on mica have accordingly been used as models for protein–gold interfacial interactions (Fig. 2). Furthermore, it should be noted that, when developing models to interpret voltammetric data, even electrodes with surface regions as seemingly pristine as that depicted in Fig. 2 are at least partially polycrystalline/disordered (perhaps $< 40\%$ of the surface is single crystal in nature) in other regions of the electrode (not shown). The need to extrapolate SPM data obtained at atomically-flat parts of the surface to the polycrystalline surfaces used in voltammetric studies represents a limitation of present SPM voltammetric investigations. The inherent mobility of biomolecules on an electrode surface presents a second significant, though solvable, problem in attaining well-defined SPM images.

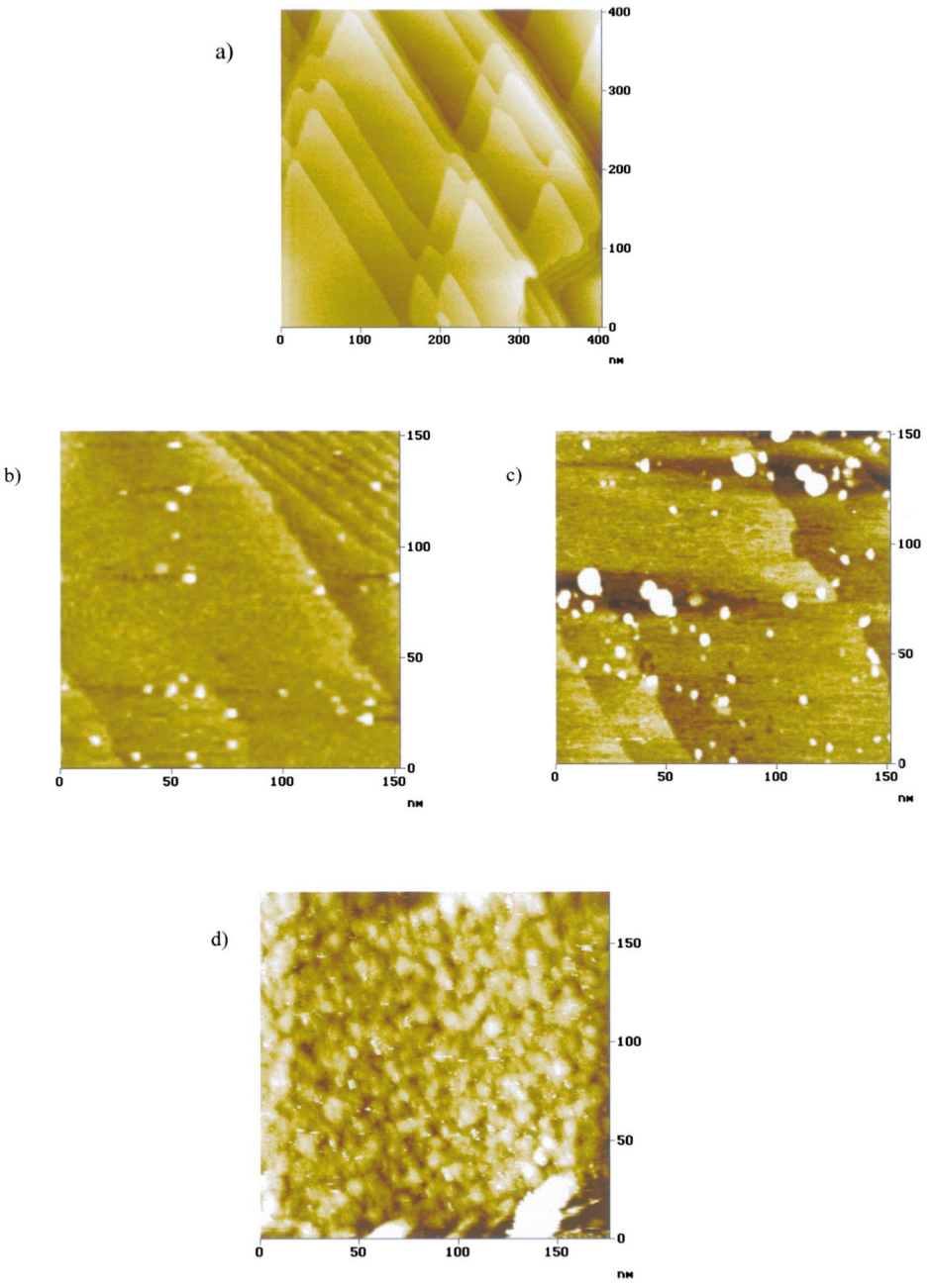
a)
400
300
200
100
0
0
100
200
300
400
nm
b)
150
100
50
0
0
50
100
150
nm
c)
150
100
50
0
0
50
100
150
nm
d)
150
100
50
0
0
50
100
150
nm

Fig. 2.

2.1.2. The adsorption of azurins

Azurins are well characterised type I or blue copper proteins which function [13,14] as electron transfer mediators at moderately positive potentials. These metalloproteins are relatively small (10–15 kDa), stable, polypeptides with little or no α-helical structure. They contain [15] a single copper atom strongly asymmetrically located in a hydrophobic core between two β sheets, at a distance of approximately 7 Å from the surface and are structurally stable over a wide range of temperature and pH. The oxidised protein from *P. aeruginosa* has a pI of 5.6 and accordingly bears a net negative charge at pH 7 [16]. The controlled introduction of residues into a protein primary structure by site-directed mutagenesis is now a relatively straightforward process [17] and many mutants of azurin have now been produced and characterised [18].

The immobilisation of wild-type azurin on gold electrodes has recently been demonstrated by scanning probe methods [19] and it was concluded that the protein chemisorbs on the substrate surface via its disulphide group (Cys3–Cys26). Though it is possible that this functionality plays a role in bonding, this methodology (i.e. studies with the wild type protein) does not allow the position of attachment/orientation of the protein at the surface to be controlled. Since the disulphide bond is an integral part of the protein structure and presumably must dissociate upon adsorption, the retention of a 'native' protein structure may accordingly be questioned. The problems associated with protein mobility in undertaking fluid SPM can be better alleviated through the use of site-directed mutagenesis as a means of non-destructive protein immobilisation [20]. The known strong interaction between thiol functions and a gold electrode surface was utilised, in a recent study [20], through the introduction of a cysteine residue into the protein surface. L-Cysteine itself is known [21,22] to bind strongly to gold via the thiol functionality. Transformation of a serine residue into a cysteine represents a conservative mutation in which no significant structural change is anticipated. Consequently, the SPM results should be readily applicable to voltammetry of the native protein.

In order to obtain images of the mutant azurin, freshly prepared, pristine gold surfaces were immersed in protein solution for several hours, then gently rinsed with deionised water and imaged by STM under water. The electrodes were found to be covered in a 'carpet' of material which, at higher magnification, could be observed to be composed of regularly-sized, quasi-spherical molecules [20] (Fig. 2(d)). Since such features were not observed if the gold substrate was immersed in deionised water and imaged under the same conditions, these were deduced to be

Fig. 2. (a) Constant current STM image of an atomically-flat single-crystalline Au[111] gold electrode surface. Set point 400 pA, bias 200 mV, scan rate 7 Hz, z-range 0–2.5 nm. (b, c) Two constant current STM data sets from a sequence of images in which the adsorption of the azurin mutant S118C on a clean gold electrode was monitored. (b) This corresponds to a period of time 3 min after the injection of $\sim$100 μl of 150 μM protein solution into the cell (to give a solution approximately 70 μM in the protein). (c) This is the same area 30 min later. Set point 1.3 nA, bias 666 mV, scan rate 6 Hz, z-scale 0–2.5 nm. (d) Constant current STM image of azurin molecules immobilised on Au[111] under 20 mM phosphate buffer, pH 7. Set point 650 pA, bias 920 mV, scan rate 8.7 Hz, z-range 0–6 nm.

azurin molecules. This conclusion was supported further by noting that the smallest resolved features are 3.5–4 nm in diameter (the long axis of the azurin molecule is approximately 3.5 nm in length). A confirmatory test of the affinity of the mutant for the gold substrate was to carry out imaging under 'true' in situ conditions; that is to image the substrate under fluid, inject the protein into the fluid cell and monitor the changes thereby observed. Significantly, the images (Fig. 2(a–c)) show a clear evolution over time, with the amount of adsorbed protein steadily increasing (in addition to noticeable agglomeration). Obviously, this time dependent (increasing) protein coverage should be incorporated into models proposed in explanation of time dependent metalloprotein voltammetry (see below). Images of individual, isolated, surface attached, azurin molecules are presented in Fig. 3.

2.1.3. Cytochrome c adsorption at gold electrodes

The images of azurin shown in Fig. 2 constitute the first in situ imaging of individual protein molecules on gold. It is worth noting that observations [23,24] made with, for example, cytochrome *c* (with no surface cysteine) suggest that affinity for a bare gold electrode surface is not inherent in all protein molecules (a solution-phase STM study of cytochrome *c* has confirmed [23] that the metalloprotein does adsorb on gold surfaces, but that this occurs with a considerable degree of aggregation and retention of mobility). Again, this feature should be incorporated into explanations of native metalloprotein voltammetry.

In considering the voltammetric implications of SPM data on metalloprotein–gold electrode surface interactions, it is important to note that it is unlikely that all proteins present on the surface are detected by the tunnelling tip during in situ experiments, i.e. it is probable, from the nature of proximal probe experiments, that a greater degree of protein coverage and agglomeration exists than is evident in the observed images. It has been confirmed [25] that tapping mode AFM (with its inherently lower lateral forces) gives a more accurate representation of protein surface coverage than is suggested by tunnelling studies. The high (essentially complete) coverage shown in Fig. 2(d) is what one can envisage as eventually being attained during the course of cytochrome *c* or azurin voltammetry at gold electrodes. That is, voltammetric scans obtained on initially placing a gold electrode surface in contact with a metalloprotein solution will be associated with sub-monolayer, or lower, coverage, whilst later (after a sufficient time) scans will be more representative of processes occurring at full monolayer coverage.

2.1.4. The adsorption of metallothionein and rubredoxin at gold electrode surfaces

Recent work carried out with all zinc metallothionein [26] has demonstrated that this non redox-active protein adsorbs, under buffered conditions, on to gold electrode surfaces and can subsequently be scanned (by STM) at exquisite resolution. Though the metalloprotein contains 20 cysteine residues, these are all involved in coordination to the metal ions and are accordingly not expected to be available in an anchoring role to the underlying substrate. A more recent in situ tunnelling study carried out on the adsorption of rubredoxin (*Clostridium pasteurianum*) at a gold electrode [27] further indicates that some metalloproteins are sufficiently stable

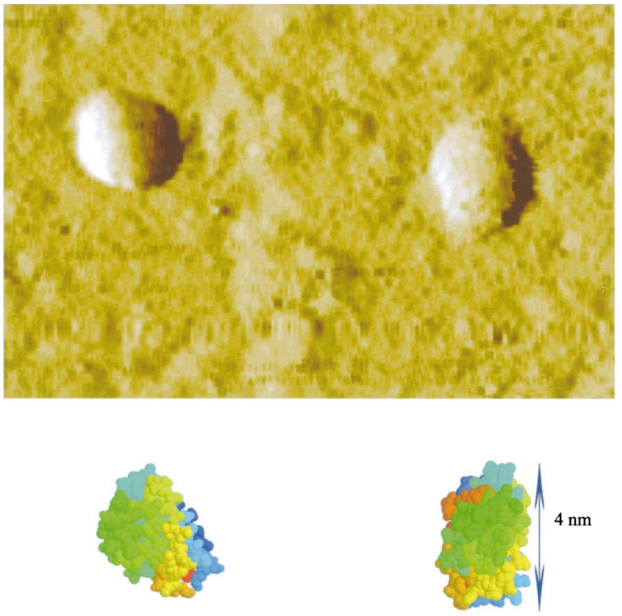

Fig. 3

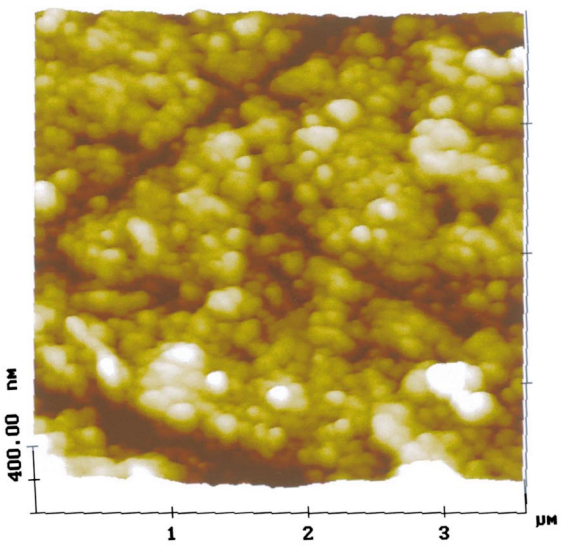

Fig. 4

Fig. 3. A comparison of a constant height image of two individual azurin S118C molecules on Au[111] with orientated, space-filling models of the protein. Image taken under deionised water with set point 940 pA, bias 770 mV, scan rate 9.4 Hz, z-range 2.5 nA and scan size 12×16 nm.
Fig. 4. Ambient contact AFM image of a polished polycrystalline gold electrode surface. Scan rate 4.5 Hz, z-range 0–400 nm, scan size 3.6×3.6 µm.

on gold electrodes for proximal probe studies to be possible in the absence of an obvious anchoring functionality (although rubredoxin, like metallothionein, does contain a surface methionine residue, the contribution of this to the process of adsorption is not known).

2.1.5. SPM characterisation of polycrystalline gold surfaces

As anticipated, polycrystalline gold electrodes, after polishing with an alumina slurry (as typically used in electrochemical studies), are seen to be far from flat on a micrometre scale. In addition to the presence of 'rounded hill' surface features, 100–200 nm in diameter (r.m.s. roughness 15–30 nm), defects and polishing scratches are also evident (Fig. 4). In view of the relative complexity and roughness of these surfaces, the adsorption of protein at polycrystalline gold electrodes cannot be studied directly. One would, however, expect that protein adsorption/aggregation on these rough surfaces would be even greater than that observed on atomically-flat single crystalline electrodes of the same nominal geometric area.

2.1.6. SPM characterisation of chemically modified gold electrodes

The rate of electron transfer between redox proteins in their natural environment is high and central to this is believed to be a 'recognition process' by which the two colliding molecules interact favourably and strongly, though reversibly. It was subsequently shown [7], that fast electron transfer between a redox protein and a solid electrode surface could be achieved, provided that surface is functionalised in a way which allows specific, favourable, reversible binding of the redox protein, i.e. a protein–electrode surface recognition process. Central to the action of these surface-modifying molecules appears to be the maintenance of protein structure/stability in a configuration where the protein is sufficiently close to the electrode so as to allow rapid electron transfer between the surface and the protein redox site. The surface modifiers also appear to prevent direct adsorption of the metalloprotein on to the bare electrode surface. Modification of a gold electrode surface with pyridine derivatives, for example [2], transforms the surface from being normally hydrophobic to hydrophilic. Such a surface appears to be able to 'recognise' and bind suitably charged redox proteins such as cytochrome *c* and in so doing 'promote' the observation of their direct electrochemistry. A basic mechanism for of the interaction between the 'promoter' (facilitator[1]) and cytochrome *c* has been proposed [28–30] (Fig. 5(a,c)[2]): diffusion of metalloprotein to the surface, adsorption to the facilitating adlayer in a favourable orientation, electron transfer, desorption and then diffusion of the protein away from the electrode surface. The second step in particular, is crucial and governed largely by electrostatic forces.

[1] Since 'promoter' is a term now much used in molecular biology, these adsorbed molecules are better referred to as 'facilitators'.

[2] It should be noted that the figures used to depict these adlayer-protein interactions are obviously idealised models. The electrode surface, in reality (see Figs. 4 and 7), is a complex mixture of topographies. Protein-surface interactions will similarly be highly variant. The experimentally determined electrode potentials and heterogeneous electron transfer rate constants will therefore reflect a guassian distribution of all those values actually present.

A large number of 'facilitators' have been synthesised and successfully used [31,32] (Table 1). Though it is assumed that most of these molecules form condensed, well-defined monolayers on gold electrode surfaces, knowledge of these structures is not adequate because their molecular orientation/arrangements on the electrode and their interactions with a protein are difficult to determine via spectroscopic techniques. Recently [33,34], however, it has become possible to image, at high resolution, the arrangements formed by these molecules on gold electrode surfaces by STM (Figs. 5(b) and 6(a)).

Fig. 6(b) shows an ECSTM image of a single crystal gold electrode surface modified with 4,4′-dithiobipyridine 3 min after the addition of approximately 200 μl of 200 μM cytochrome *c* solution in to the STM cell. Though imaging was commonly streaky and unstable on re-attaining feedback (characteristic of protein-tip interactions [35]), the surface features of the 4,4′-dithiobipyridine modified electrode clearly change on addition of the cytochrome and it was possible, on some occasions, to resolve small structures, the smallest of which could be assigned to individual cytochrome molecules. Though these observations are consistent with the

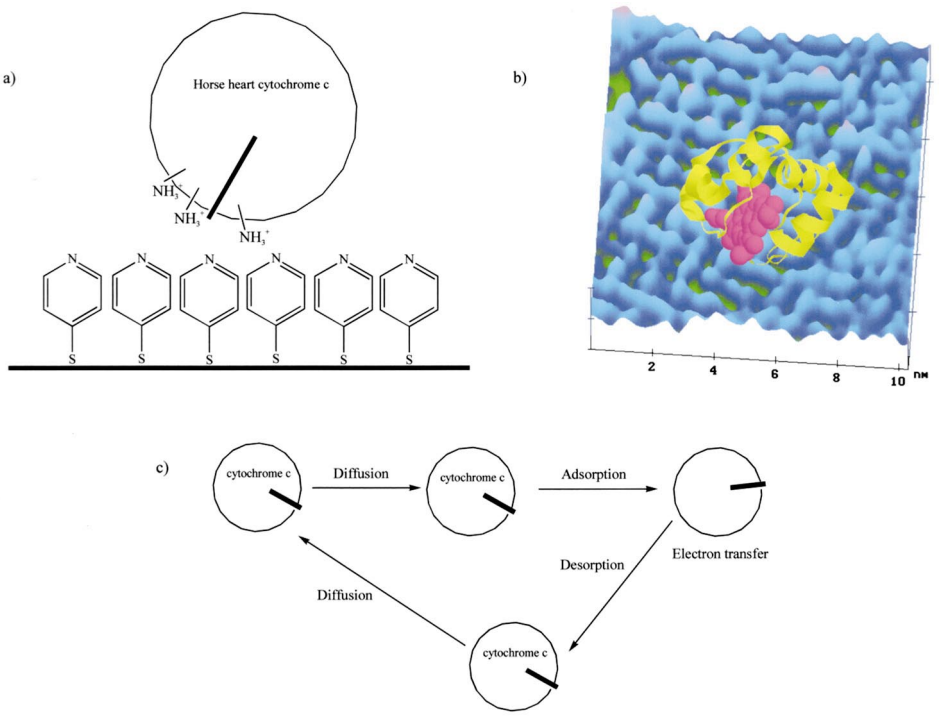

Fig. 5. (a) Schematic representations of the interaction between a 4-pyridyl thiolate modified gold electrode surface and the cytochrome *c* molecule. Shown on the right (b) is an STM image of a facilitating 2-mercaptopyrimidine adlayer on gold (with the protein structure superimposed). (c) A schematic depiction of the processes associated with redox protein electron transfer at an electrode/electrolyte interface.

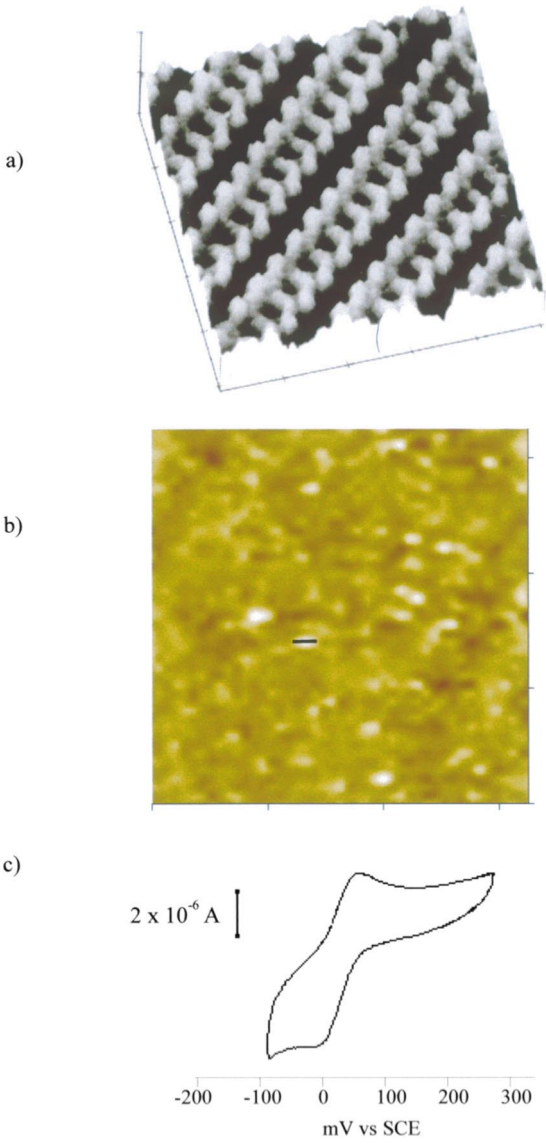

Fig. 6. (a) High-resolution STM image of a 4,4′-dithiobipyridine adlayer on Au[111] in 0.05 M $HClO_4$ solution. Set point 2 nA, bias 300 mV, z range 0–0.32 nm, scan size 5×5 nm. Reproduced with permission from Ref. [34]. (b) Constant current electrochemical STM image of an 4,4′-dithiobipyridine modified Au[111] electrode approximately 3 min after the addition of approximately 100 μl of 200 μM cytochrome c solution to the STM cell. Set point 250 pA, bias 950 mV, scan rate 5.8 Hz. Scale bar 4 nm. The simultaneously recorded voltammetric response (c) is also shown (scan rate 21 mV s^{-1}).

electrode–facilitator–protein model shown in Fig. 5(b), it is not clear whether the adsorbed metalloprotein sits on top of or slowly displaces the facilitating adlayer.

2.2. SPM characterisation of graphite electrodes

2.2.1. Highly orientated pyrolytic/basal plane graphite electrodes

Highly orientated pyrolytic graphite (HOPG) is a substrate commonly used in SPM because it is easily cleavable to produce a surface which is atomically flat over several square micrometres (Fig. 7(a)). Though popular because of this, the surface is highly hydrophobic in its 'native' state and hence not generally amenable to (non-destructive) surface interactions with biomolecules. Despite this, HOPG has been used successfully in the AFM/STM imaging of proteins and enzyme and is equivalent to the basal plane graphite (BPG) surfaces commonly used in electrochemical investigations. High-resolution STM images of horse-heart cytochrome *c*, deposited on a HOPG surface, are presented in Fig. 8. Individual molecules (with dimensions very close to those determined by X-ray diffraction) of the cytochrome

Table 1
Species which are able to facilitate electron transfer between redox proteins/enzymes and a gold electrode surface (these include thiol-based organic molecules [31], peptides [55], adatoms [56] and colloidal gold [57])

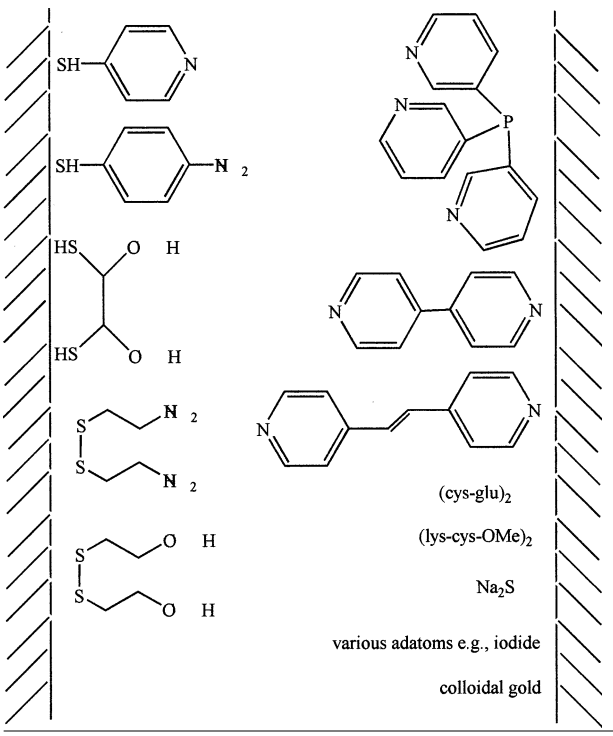

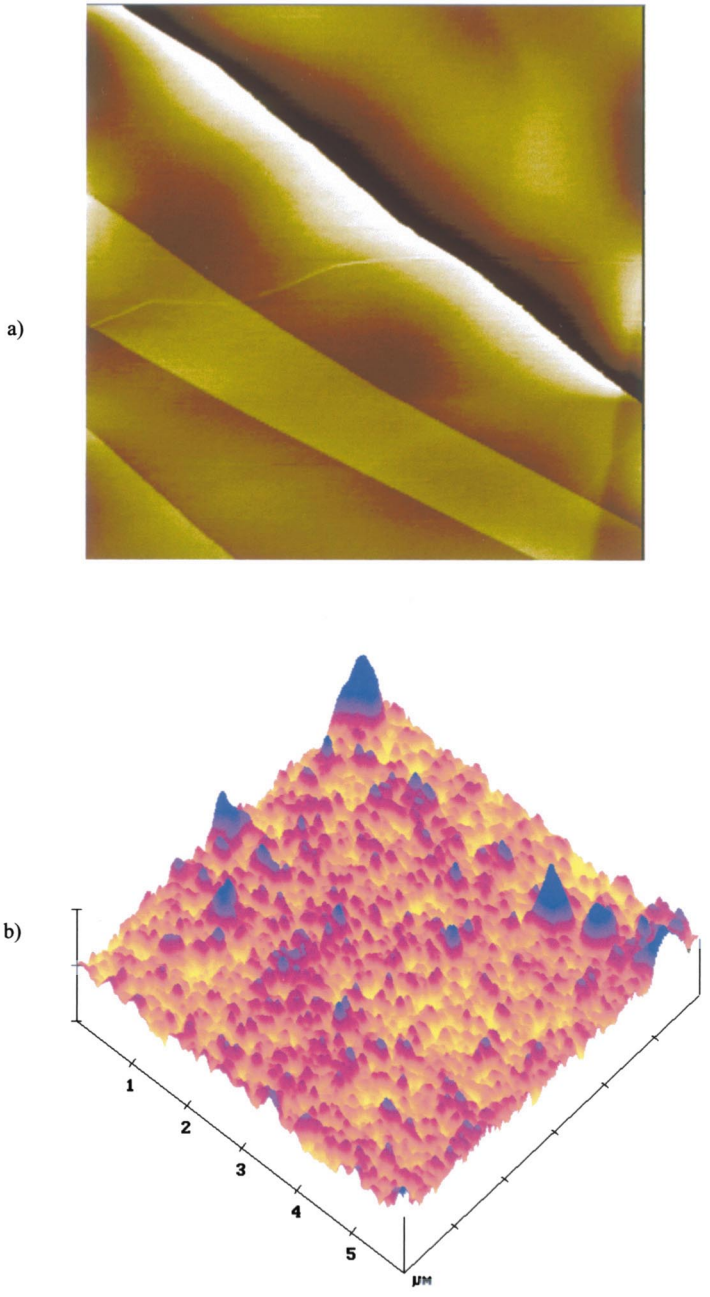

Fig. 7. (a) A constant current STM image of the single crystal highly orientated pyrolytic graphite electrode surface. Set point 1 nA, bias 200 mV, scan rate 5 Hz, z-range 0–4 nm, scan size 2×2 μm. (b) Low-resolution contact AFM image of a polished EPG electrode surface. Scan rate 6 Hz, z-range 0–250 nm, scan size 6×6 μm.

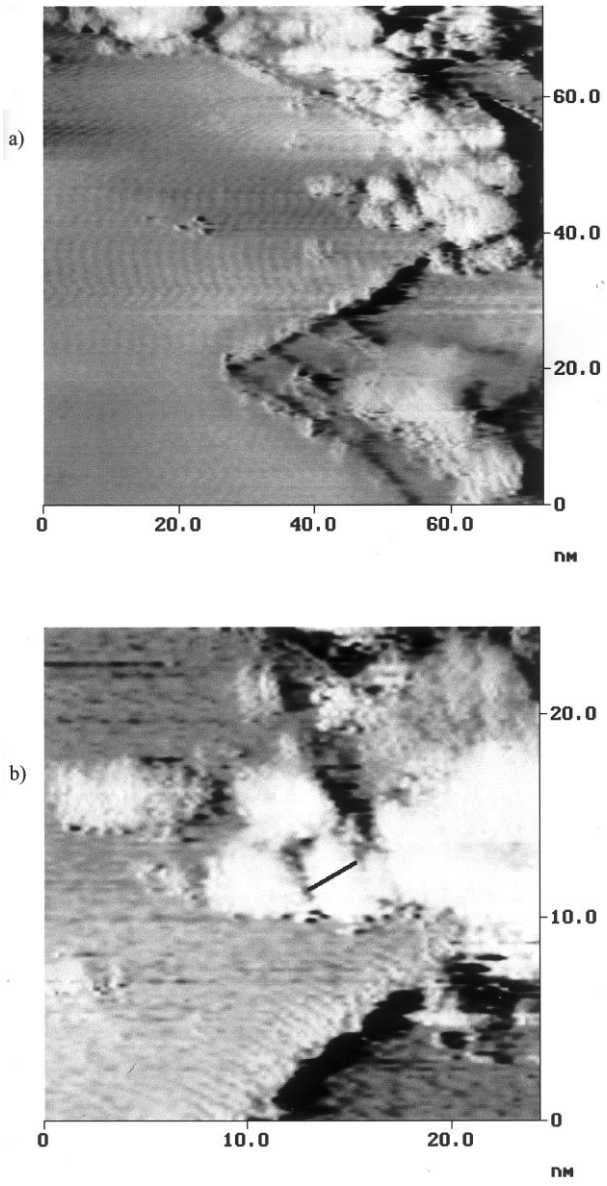

Fig. 8. Constant current ambient STM images of molecules of horse-heart cytochrome *c* deposited from aqueous solution onto a freshly cleaved HOPG electrode surface. Of particular relevance is the obvious preferential accumulation of the protein at step edges on the, otherwise pristine, surface. Set point 1.0 nA, bias 100 mV, scan rate 8.7 Hz, *z*-range 0–5 nm, scan size 80 × 80 nm. Three individual cytochrome molecules are shown in (b). Tunnel parameters the same as in (a), scan size 25 × 25 nm. Scale bar 3.5 nm.

are clearly evident. Interestingly, and of likely electrochemical significance, the protein molecules preferentially aggregate at defect sites and step edges in the surface (Fig. 8(a)) which are likely to possess hydrophilic, 'anchoring' oxygen-based functionalities (see Section 3.2). That is, the protein is able to adhere to these groups as it slides across the otherwise 'slippery' hydrophobic surface on deposition from an aqueous solution. An equivalent situation is thereby observed, on at least part of the electrode surface, to that at a deliberately modified gold electrode surface.

2.2.2. Edge plane graphite electrodes

Edge plane graphite electrodes used in voltammetric studies are, in stark contrast to HOPG, very rough (Fig. 7(b)). The act of polishing adds further to this in the creation of surface scratches of variable diameter and depth. Further to this, EPG surfaces, polished in air, possess a high density of various carbon oxide functionalities [7] and approach the situation depicted in Fig. 5 at a modified gold electrode (Section 3.2).

3. Relevance of SPM data to metalloprotein voltammetry

SPM observations demonstrate that all metalloproteins studied to date interact with electrode surfaces to some degree. Simple, diffusion based, voltammetry cannot accordingly be expected. Traditionally, authors of most metalloprotein papers have attempted to find solution-phase conditions that give a diffusion controlled response which can be modelled by Eq. (1). Under these ideal conditions, with a macrodisc electrode and linear diffusion, the following voltammetric conditions (based on the standard Butler–Volmer treatment) are expected for a reversible process;

$$\mathrm{Ox} + n\mathrm{e}^- \overset{E^\circ,\ k_s,\ \alpha}{\rightleftharpoons} \mathrm{Red} \tag{1}$$

$$I_p = (2.69 \times 10^5) n^{3/2} c D^{1/2} v^{1/2},\ \Delta E_p = 56/n \text{ mV at } 25^\circ\mathrm{C},$$

$$I_{pa}/I_{pc} = 1.0 \text{ and } E_{1/2} = [E_{pa} + E_{pc}]/2$$

where I_p is the peak current, E° is the standard reversible potential (more rigorously in practice this will be the standard formal potential as voltammetric experiments on proteins are rarely undertaken at unit activity or 25°C), E_p is the peak potential, I_{pa} and I_{pc} are the anodic and cathodic peak potentials respectively, $E_{1/2}$ is the half wave potential and E_{pa} and E_{pc} are the oxidation and reduction peak potentials respectively, v is the scan rate in V s^{-1}, c is the bulk solution protein concentration in mol cm^{-3}, D is the diffusion coefficient in cm^2 s^{-1}, k_s is the heterogeneous charge transfer rate constant in cm s^{-1}, α the charge transfer coefficient, Ox and Red the oxidised and reduced forms of the metalloprotein respectively and n is the number of electrons transferred [36].

If significant metalloprotein interactions with the surface occur, Eq. (1) is no longer valid and several mechanistic possibilities are then expected:

1. A mixture of diffusion controlled (Fig. 9(a)) and surface confined behaviour. Wopschall and Shain have considered [37,38] this case and, depending on the adsorption isotherm and the free energy of adsorption, pre- and post-waves, as well as the 'normal' waves, may be observed (Fig. 9(b)).
2. Fully surface confined behaviour, where most, if not all, of the metalloprotein is irreversibly (commonly) adsorbed in both the oxidised and reduced forms. In this case, more symmetrical shaped voltammetric waves are expected (Fig. 9(c)), with a different scan rate dependence ($I_p \propto v$) to a diffusion-controlled process. Furthermore, the surface confined reversible potential may no longer be the same as that observed for the 'solution-phase' species [46].
3. Unlike conditions 'a' and 'b', where the native protein structure is assumed to be essentially retained, metalloprotein interactions with the surface may also lead to unfolding and subsequent creation of a denatured, electroinactive, form. Structural changes of this kind may lead to blockage of the electrode surface (leading to a loss of electrochemistry in the vicinity of the native, reversible, potential) and other, electrochemically undesirable, effects. Many of these can be at least partially alleviated through the use of chemically modified electrode surfaces. In such circumstances, the theoretical models introduced by Albery et al. [30] or Honeychurch and Rechnitz [39] are expected to apply (see later).

In the remainder of this review we will show that all of the above scenarios (a)–(c) are observed.

3.1. Voltammetry at gold electrodes

3.1.1. Azurin voltammetry at bare gold electrodes

Interactions of both wild-type and S118C mutant azurins have been monitored by SPM methods. A question that subsequently arises is: what impact does this data have on our interpretation of azurin voltammetry at gold electrodes? Azurin voltammetric responses at a bare gold electrode surfaces are presented in Fig. 10(a,b) and they are clearly not of the simple diffusion-controlled kind. The cyclic voltammetric response of the wild-type protein, is transient at bare, unmodified, gold electrode surfaces [19,40] (Fig. 10(a)). Thus, with a repetitive cycling of potential (increasing electrode contact with the protein), the initially peak shaped curve decreases in height and changes to a more sigmoidal shaped response. This time dependence implies that adsorption of azurin on to the electrode, as implied by the discussed STM study, gradually blocks the surface so that the expected linear diffusion controlled process is not detected when high surface coverages are present. In contrast, the electrochemistry of the S118C mutant is far more stable when subject to continuous scanning experiments (Fig. 10(b)). In this case, however, a scan rate study is consistent (peak height proportional to scan rate) with the electroactive species being surface-confined. The shape of the current–potential curve is also characteristic of surface confined, rather than solution phase voltammetry and the potential where this stable process is detected is well removed from the solution phase reversible value (approximately 100 mV more positive). The

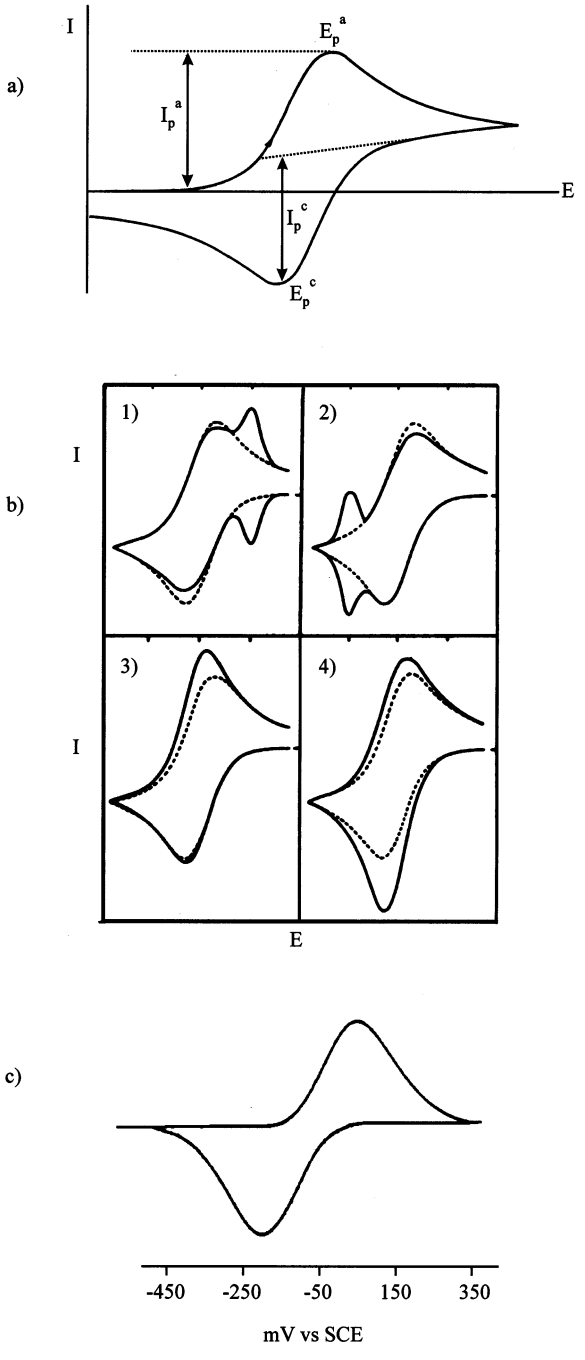

Fig. 9.

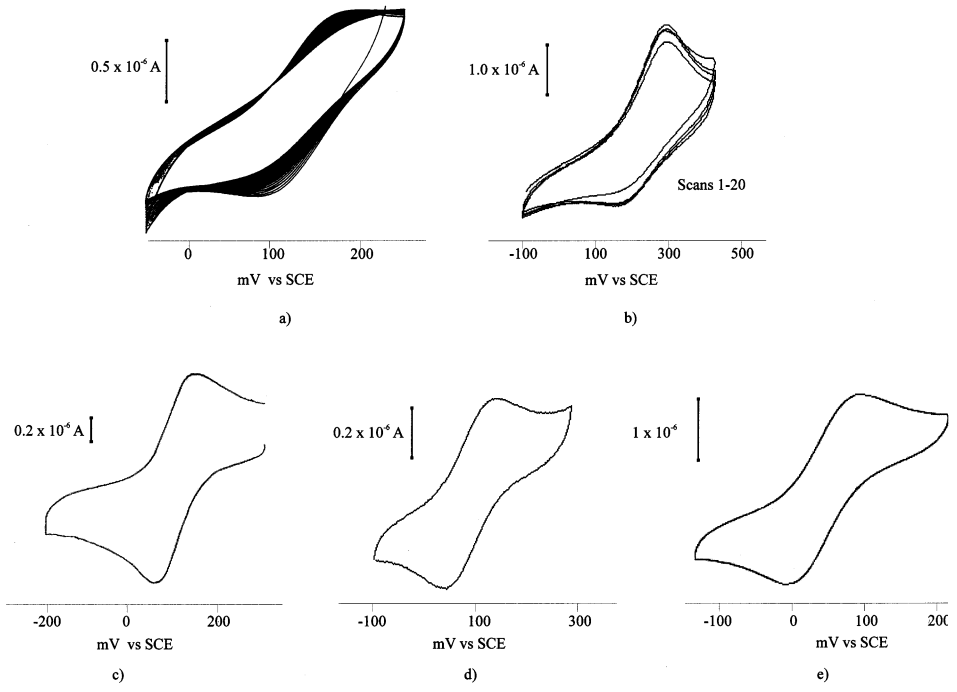

Fig. 10. (a) Consecutive scans of 138 μM *P. auruginosa* azurin wild-type in 50 mM ammonium acetate, pH 4.7, at a polycrystalline gold electrode, at 10 mV s^{-1}. The signal decays exponentially with time. (b) Electrochemical response of 70 μM azurin S118C at a polycrystalline gold electrode in 20 mM HEPES buffer, pH 7, 100 mM KCl, at 20 mV s^{-1}. Note that the midpoint potential has shifted approximately 100 mV to the positive of that observed for the protein at an EPG electrode. (c) Electrochemical response of 100 μM azurin wild-type at a polished EPG electrode, in 20 mM HEPES buffer, pH 8, 100 mM KCl, at 10 mV s^{-1}. (d) Electrochemical response of 60 μM azurin S118C at a polished EPG electrode, in 20 mM HEPES buffer, pH 7, 100 mM KCl, at 20 mV s^{-1}. (e) Electrochemical response of azurin wild-type in 50 mM phosphate buffer, pH 6, at a 4,4′-dithiobipyridine modified polycrystalline gold electrode, at 20 mV s^{-1}.

potential at which the voltammetric responses of wild-type azurin occur also appear to be significantly removed (about 80 mV positively) from the solution phase reversible value.

The importance of the S118C cysteine residue in the mutant protein affinity for gold was demonstrated through the observed effect of blocking this residue by reaction with β-alanoyl maleimide [20], and noting the significant decrease in

Fig. 9. (a) An idealised cyclic voltammogram for a reversible electrochemical process. Initially, only the oxidant is present in solution. (b) Theoretical cyclic voltammograms for electrode processes involving adsorption: (1) Reactant weakly adsorbed. (2) Product weakly adsorbed. (3) Reactant strongly adsorbed. (4) Product strongly adsorbed. Dashed lines indicate behaviour for uncomplicated Nernstian charge transfer (reproduced from Ref. [37]). (c) Baseline subtracted voltammetric response of *Pseudomonas auruginosa* azurin at 500 V s^{-1} immobilised on a pyrolytic graphite electrode surface, at 0°C (reproduced from Ref. [46]).

voltammetric peak height. Since the S118C response is stable to continual cycling, the adsorption must occur in such a way that electron transfer between the copper centre and the electrode remains possible, and indeed that, the native protein structure is largely retained in such a state. The S118C voltammetric behaviour on gold may be related to the location of the cysteine residue in the adsorbed state; the adjacent residue (117) is thought [41] to lie on the electron transfer pathway from the copper centre to co-proteins of azurin. This may explain why the half wave potential for the surface-confined process was shifted by approximately 100 mV positive of the reversible potential expected if a solely solution-phase process had occurred. Nevertheless, the time dependence of the native azurin response and the lack of any response at the reversible potential with S118C, despite the high solution concentration, implies (in both cases) that adsorbed azurin partially blocks or inhibits the diffusion controlled process that would otherwise be expected at a bare gold electrode surface if no irreversible interactions occurred. Clearly, modelling of azurin voltammetry at gold needs to accommodate both the time dependence of the wild type response and the potential shifted voltammetry of the adsorbed S118C species. Additionally, a model should explain why voltammograms at carbon electrodes (and chemically modified gold electrodes — see below) are diffusion controlled and relatively simple in comparison to those observed at bare gold electrodes.

In summary, microscopy observations of both the wild type and S118C mutant protein are consistent with specific adsorption of the copper protein under the appropriate conditions [19,20]. In the case of the wild type protein, the disulphide bridge is believed to be central to the interaction with gold, while in the case of the S118C protein, the molecule was selectively anchored to the underlying substrate through the application of mutagenesis. The impact of this latter methodology on voltammetric observations subsequently made at the gold electrode is to give a mid-point potential significantly removed in value from the reversible solution phase value at this pH [42]. Furthermore, both the scan rate dependency and wave shapes are characteristic of the electroactive moiety being strongly confined to the surface.

Strong adsorption of a protein can be prevented by modification of the underlying bare gold electrode surface. Thus the voltammetric response of wild type azurin at a 4,4′-dithiobipyridine modified surface shown in Fig. 10(e) corresponds to an almost classic example of a reversible, diffusion controlled response at a potential very close to the predicted reversible (solution phase) value. Under such conditions, it is likely that the dithiobipyridine is preferentially adsorbed on the gold surface (strongly and reversibly, Fig. 6(a)) and effectively blocks specific adsorption of the copper protein on the gold. Under these conditions, the electron transfer models (Fig. 12(a)) [30,39] could be expected to apply, with the protein diffusing to and away from the facilitating adlayer. Azurin (native or S118C) voltammetry at such chemically modified gold electrodes is diffusion controlled at low scan rates, with peak-to-peak separations of 70 ± 10 mV s^{-1} at scan rates < 100 mV s^{-1} and concentrations in the 0.1 mM range. The voltammetry observed at (oxygen functionalised) EPG electrodes for both wild-type and S118C azurin is, in fact,

remarkably similar to that observed at the chemically modified gold electrode surface (Fig. 10(c,d)) and, again, it is likely that the presence of the spontaneously functionalised surface serves to minimise irreversible protein adsorption.

3.1.2. Cytochrome c voltammetry at bare gold electrodes

SPM studies confirm that cytochrome *c*, like azurin, interacts strongly with gold surfaces and that chemical modification serves to minimise the extent, or at least rate, at which this occurs. Studies carried out at bare gold electrodes thus may not be expected to provide a diffusion-controlled response. A recent study has, however, confirmed [43] that cytochrome *c* may give such responses at an unmodified surface. This is only sustained, however, for relatively short periods of time after the surface comes in to contact with the protein solution, i.e. the response is transient or, as is the case with azurin, changes from a peak shaped (linear diffusion dominant) to a sigmoidal shaped (radial diffusion dominant) response with a concurrent decrease in faradaic current (Fig. 11(c)). The transient voltammetry at bare gold electrodes typically occurs at potentials close to the half wave (reversible) value of the native protein (10 mV vs. SCE) [44]. The SPM data and a microscopic model are consistent with these voltammetric observations; the electrochemical response at a bare surface is considered to be transient due to the self-blocking (based largely on repulsive electrostatic forces) of the electrode by adsorbed forms of the protein [43].

3.1.3. Cytochrome c voltammetry at modified gold electrodes

The almost concurrent demonstrations by Yeh and Kuwana [3] and Eddowes and Hill [2] of cytochrome *c* voltammetry at functionalised electrode surfaces paved the way for modelling in which surface chemical functionalities were proposed to interact specifically, but reversibly, with lysines on the cytochrome surface (in a region close to the exposed haem edge) [28,29]. Subsequent studies proposed [30] that three mechanistic steps may contribute to such voltammetry; adsorption, electron transfer, and desorption (Fig. 5(c)). Such models are applicable to a range of gold modified surfaces [31] at which well-defined faradaic responses, where peak height varies linearly with $v^{1/2}$, are observed. Such voltammograms, then, have a dominant linear diffusion component (see also responses at carbon electrodes below), though, almost invariably, non-ideality is observed at scan rates $> \sim 100$ mV s^{-1}.

In the cytochrome *c* data presented in Fig. 6, one should note that the simultaneously acquired, close to diffusion-controlled, voltammetric response (Fig. 6(c)) is obtained from the entire electroactive surface area (and its inherent variable topography), while the image shown in Fig. 6(b) is confined to a specific 65×65 nm region. Significantly, in order for the molecules to be imaged, they must, during the time scale of the scan (at least), be stationary or immobilised (adsorbed strongly). Thus, it may be concluded that cytochrome *c* either displaces the facilitator molecules (and adsorbs on the underlying gold) or strongly interacts with the adlayer. The protein voltammetry observed when using these ex situ modified electrodes typically decays with time under the conditions with which the ECSTM

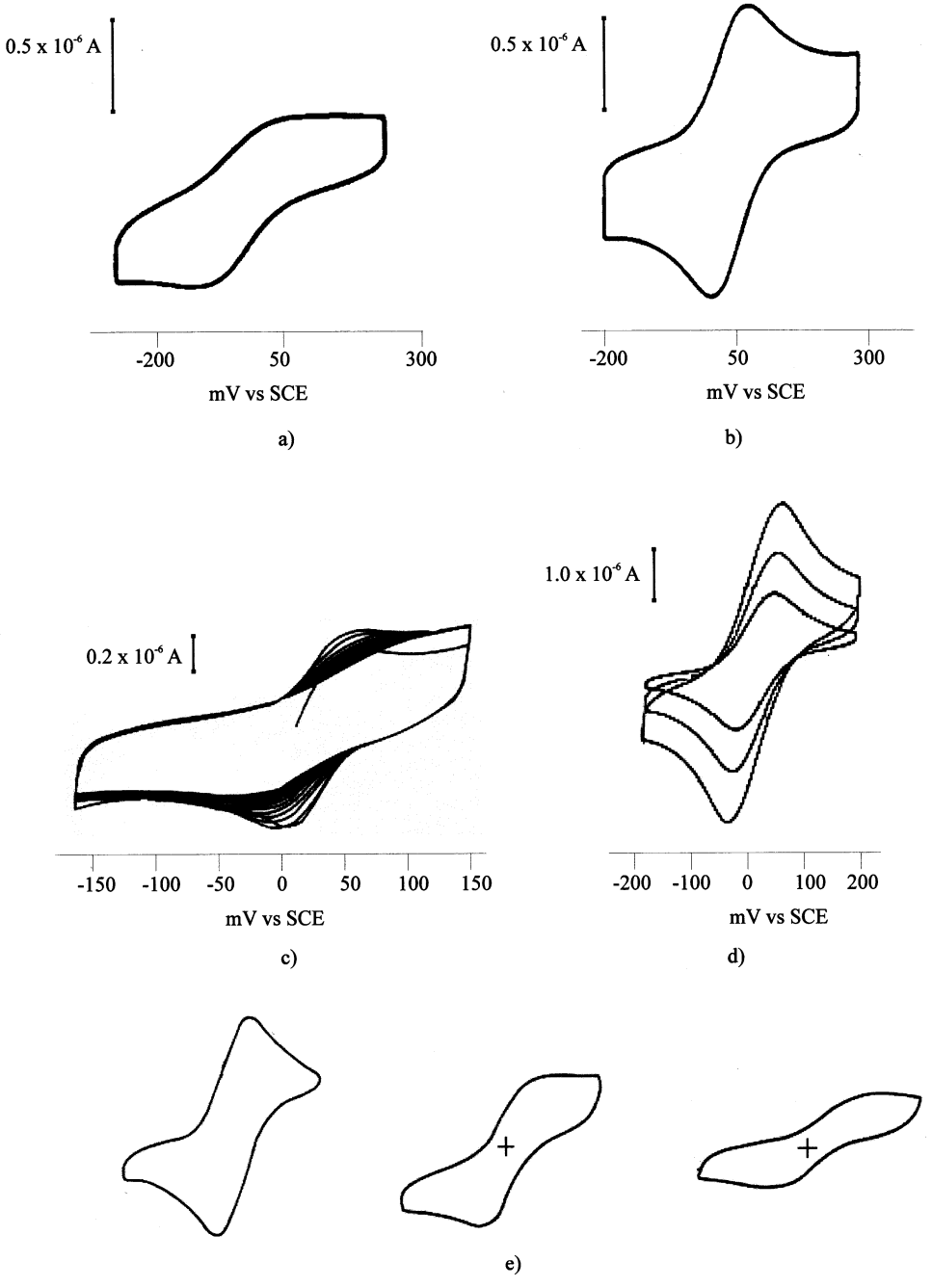
0.5 x 10-6 A
-200
50
300
mV vs SCE
a)
0.5 x 10-6 A
-200
50
300
mV vs SCE
b)
0.2 x 10-6 A
-150
-100
-50
0
50
100
150
mV vs SCE
c)
1.0 x 10-6 A
-200
-100
0
100
200
mV vs SCE
d)
e)

Fig. 11.

images were obtained (Fig. 11(e)), i.e. the adsorption of a facilitator molecule is not necessarily a wholly irreversible process. That is, species may be present in the solution phase (perhaps the protein itself) which are themselves able to strongly adsorb and in so doing these may displace the promoting adlayer (leading to electrode blockage at the sites concerned). The initial peak-shaped voltammetric responses observed subsequently become increasingly sigmoidal in appearance, as the process of diffusion effectively becomes radial, before finally disappearing altogether. Desorption of the facilitating adlayer may occur if the solution above the modified electrode surface is free of the molecule. It is accordingly not surprising that cytochrome *c* voltammetry is observed to be sustained for a longer period of time if the facilitator is present in solution and thereby more able to 'compete' with the protein for occupancy of the electrode surface as in the study [30] of the use of 4,4′-bipyridyl as a facilitator.

3.2. Voltammetry at carbon/graphite electrodes

3.2.1. Graphite electrodes

Pyrolytic graphite electrodes, polished in air, possess surface layers of various carbon oxide functionalities. These surfaces accordingly act as 'spontaneously modified' electrodes, with the basal surface being partially covered and the edge plane surface heavily functionalised (X-ray photoelectron spectroscopy has confirmed [45] that the basal surface is largely devoid of oxygen (O/C ratio ~ 0.02) while the polished edge plane surface is oxygen rich (O/C ratio ~ 0.33)). The latter electrode surface is accordingly conducive to the observation of good, quasi-reversible and stable voltammetric responses with cationic proteins, such as cytochrome *c*, where only small faradaic currents are typically observed with the same proteins at a basal electrode [8].

3.2.2. Azurin voltammetry at graphite electrodes

Azurin bears a net negative charge in the neutral pH region but this is low and the voltammetry observed at these functionalised carbon surfaces is typically excellent and occurs close to the reversible potential (Fig. 10(c)) — note the analogy of the voltammetry to both cytochrome *c* and azurin at chemically modifed gold electrodes. Thus, at an oxygen functionalised surface, peak current is a linear function of the square root of scan rate and the peak-to-peak separation indepen-

Fig. 11. Electrochemical response of 0.15 mM horse-heart cytochrome *c*, in 5 mM Tricine, 0.1 M NaCl, pH 8, at (a) a freshly cleaved BPG electrode, (b) a polished EPG electrode. Both scans recorded at 20 mV s^{-1}. (c) Electrochemical response at a bare polycrystalline gold electrode of 100 μM horse-heart cytochrome *c* in 0.1 mM potassium phosphate buffer, pH 7, at 20 mV s^{-1}. Scanning was initiated as soon as the electrode came into contact with the protein solution. (d) Electrochemical response of 0.4 mM horse-heart cytochrome *c* in 20 mM potassium phosphate buffer, pH 7, at a polycrystalline gold electrode modified with 4,4′-dithiobipyridine. Scans at 20, 50 and 100 mV s^{-1} are shown. (e) Cyclic voltammetry, at 20 mV s^{-1}, of 400 μM cytochrome *c* in 20 mM potassium phosphate/100 mM $NaClO_4$, pH 7, at a 4,4′-dithiobipyridine modified gold electrode. The effects of an increasing displacement of the promoting adlayer by mercaptoethylamine is shown on moving from left to right. Reproduced from [52].

dent of scan rate up to 50 mV s^{-1}. Functionalities present on the polished EPG surface facilitate the electrochemistry of this (and other) metalloprotein so that the shape of the subsequently observed voltammetric waves is characteristic of the dominant mode of mass transport being diffusion of the protein to the modified part of the surface at which it exchanges electrons. The higher the coverage of 'suitable' (docking) functional groups, the more linear the process of diffusion. SPM studies indicate, however, that some degree of metalloprotein adsorption occurs at unfunctionalised regions of the surface which, again, is consistent with observations that voltammetry becomes increasingly less ideal as solution contact times (or protein concentrations) increase.

At higher scan rates (and solutions of typically 100 μM protein concentration), the voltammetric behaviour of azurin at EPG electrodes departs from an idealised diffusion controlled response (the current is no longer proportional to $v^{1/2}$), suggesting a small, but significant, adsorbed component to the voltammetry. Conversely, in very dilute systems, the voltammetry at very fast scan rates is observed to be almost exclusively surface confined (Fig. 9(c)) [46]. If fast scan rates are used in surface-confined studies any residual diffusion component is typically lost. The, almost purely, diffusion controlled responses, with mid point potentials at the reversible value, for the S118C mutant and wild type azurin at polished EPG are shown in Fig. 10(d and c), respectively.

3.2.3. Cytochrome c voltammetry at carbon electrodes

Since it is a highly positively charged protein at pH 7, cytochrome *c* exhibits very good, reversible, voltammetry at negatively charged polished EPG surfaces (Fig. 11(b)). Thus, as for azurin, voltammograms of cytochrome *c* at carbon electrodes have a dominant diffusional component at low scan rates. In the absence (or low coverage) of surface functionalities (BPG or HOPG), the voltammetry is either sigmoidal (radial diffusion) and poorly defined (Fig. 11(a)) or else the response is not detectable above the background (HOPG) [47].

4. Discussion

Data obtained by scanning probe microscopy lead to the conclusion that interactions of metalloproteins with gold and carbon electrode surfaces are significant and that the theories which should accordingly be applied to the voltammetry of cytochrome *c*, azurin, and presumably that of other metalloproteins, should be based on models a or b as depicted in Fig. 12 and not on the model that has been predominantly used in the first 20 years of metalloprotein electrochemistry (where only a simple process of protein diffusion to and from a uniform electrode surface

is considered, see Eq. (1))[3]. Interestingly, entirely analogous models appear to be equally valid for chemically modified gold electrodes (the deliberate addition of a facilitator) and carbon electrodes (where the spontaneous formation of an oxygen-functionalised surface occurs on exposure to dioxygen). Furthermore, at both electrode types, multilayer, monolayer or sub-monolayer facilitator coverages may be present, depending of the exact conditions that apply to the experiment being considered. In the case of complete coverage, model a should be appropriate to describe the interfacial region, while, for partial coverage, the electrode interface exists in a form of the kind displayed in model b. Intriguingly, at unmodified and concomitantly clean gold (and presumably pure pyrolytic carbon) electrode surfaces, direct adsorption of metalloprotein occurs, leading to a blocking of the electrochemical activity of native solution (soluble) protein at the reversible potential, at least with respect to diffusion controlled processes. The theory which should be applied in such cases is based on model b (where the patches of adsorbate/protein are now electroinactive.)

An important matter to emerge from studies based on identifying the correct models to be used for theoretical calculations is the difference that the use of models a and b may make relative to traditionally used theoretical models. Conventionally, when metalloprotein is present in the solution phase, the electron transfer reaction has been treated by Eqs. (1) or (2) when written specifically in the form relevant to the proteins considered in this paper.

$$\begin{aligned} &\mathrm{Az[Cu^{II}]} + \mathrm{e^-} \overset{E^\circ,\ k_s,\ \alpha}{\rightleftharpoons} \mathrm{Az[Cu^{I}]} \\ &\mathrm{Cyt\ \ } c\mathrm{[Fe^{III}]} + \mathrm{e^-} \overset{E^\circ,\ k_s,\ \alpha}{\rightleftharpoons} \mathrm{Cyt\ \ } c\mathrm{[Fe^{II}]} \end{aligned} \tag{2}$$

If the relations in Eq. (2) are valid, then cyclic voltammetry with an electrochemically reversible process at a macrodisk electrode under (linear) diffusion controlled conditions;

1. The average of the reduction and oxidation potentials should be independent of scan rate and equal to the reversible potential.
2. ΔE_p should have a scan rate independent value of $56/n$ mV at 25°C.
3. Peak current should be proportional to the square root of scan rate [36].

However, if model a, implied by the discussed SPM, is correct, and electron transfer occurs at the modified surface, which is a significant distance from the electrode surface, then the protein does not experience the full force of the potential applied to the electrode surface and shielding occurs (Fig. 12(a)). The extent to which the normally-assumed conditions of a bare electrode are altered is determined by the nature of the double layer, which in turn is a function of the electrolyte present, the point of zero charge, and hence also the electrode material. The problem of reversible voltammetry occurring at the boundary of a chemically

[3] During STM investigations of protein adsorption it is not possible to easily separate the contributions of surface physical and chemical properties from possible effects of the surface electric field. Since the fields typically present in electrochemical investigations will be of the same magnitude as those present during the discussed tunnelling experiments, we believe the conclusions drawn from this study remain valid.

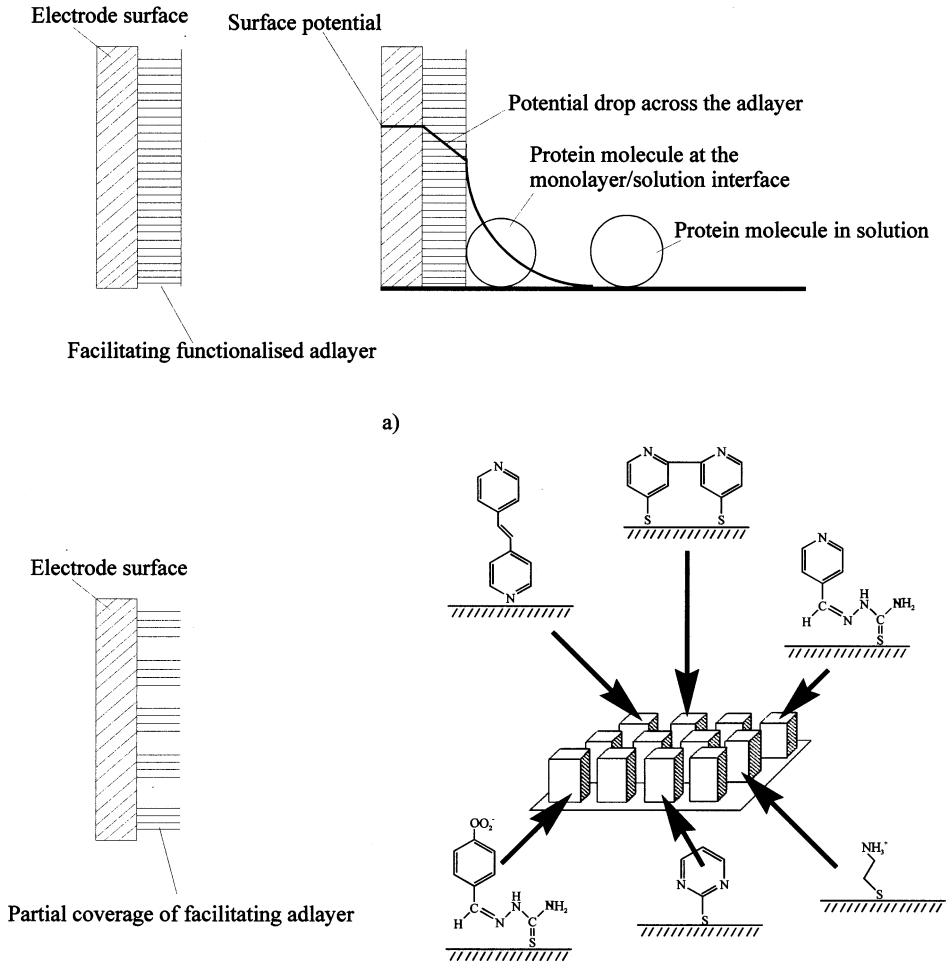

Fig. 12. (a) Model a; the electrode surface area is both flat and uniformly electroactive over its entirety. In the case of the surface being modified with a facilitating adlayer, the drop in potential across this must be taken into account when interpreting subsequently obtained protein voltammetry. (b) The electrode surface is functionalised, but not uniformly. Electron transfer accordingly takes place preferentially at localised sites on the surface. A schematic illustration of an array of adsorbed facilitating molecules on a gold electrode surface. The proven or anticipated mode of adsorption is given for each of the surface modifiers: clockwise from top centre; 4,4′-bipyridyldisulphide, PATS-4 (4-pyridylaldehyde-thiosemicarbazone), CATS-4 (thiosemicarbazone; 4-carboxybenzaldehyde), 2-mercaptopyrimidine, 2-mercaptoethylamine, 1,2-bis(4-pyridyl)ethylene. Reproduced from Ref. [54].

modified surface has been treated by Honeychurch and Rechnitz [39]. A range of subtle differences arise from use of theory applicable to model a, relative to the usually considered case where reversible electron transfer occurs at distances very close to the bare electrode surface. In particular, simulations based on model a

reveal that ΔE_p values can be significantly greater than $56/n$ mV and, for example, could easily be in the 65–70 mV range commonly reported in cyclic voltammetry experiments undertaken on metalloproteins at macrodisk electrodes. However, values of ΔE_p greater than $56/n$ mV have normally [48] been ascribed to a slow rate of electron transfer, which is said to correspond to the quasi-reversible model first theoretically considered in detail by Nicholson [49] (indeed, for many years, it was almost standard practice in the field of metalloprotein voltammetry to use the theoretical tables or working curves provided by Nicholson to calculate rates of electron transfer from the measured ΔE_p values). In contrast, use of model a (supported by SPM) could lead to the conclusion that such processes are reversible as opposed to quasi-reversible. That is, the true rates of heterogeneous electron transfer could be significantly greater than implied by the published values based on the use of a conventional, but probably incorrect, theoretical model. Furthermore, the use of average values of peak potentials to calculate reversible potentials and of the Randles–Sevcik equation to calculate diffusion coefficients is also likely to introduce errors, as these equations do not rigorously apply if model a is applicable.

Intriguingly, Miller et al. have deliberately employed gold electrodes coated with well-defined self assembled monolayers of thiols of variable chain length and studied the voltammetry of cytochrome *c* (present in the solution phase) at this form of modified electrode [50]. The results show that, for electrodes modified with short chain length thiols, such as $HO(CH_2)_3SH$, well-defined, almost reversible, diffusion-controlled, voltammograms are observed (as with 4,4′-dithiobipyridine-modified or oxidised carbon electrodes). With long chain length thiols, such as $HO(CH_2)_{11}SH$, very drawn out waves with a flattened peak shape (as predicted by Marcus theory) are observed. The interested reader may thus usefully consult published work [30,39,51] to fully appreciate the implications of voltammetric features which may arise and which are related to the use of monolayer level coverages of facilitators or surface modifiers.

Voltammetric studies have also been carried out with cytochrome *c* immobilised on carboxylate terminated thiols of variant chain length on gold electrodes. These systems have been used in the production of well-defined, surface-confined diffusionless voltammograms [50]. Thus, when the electrode is modified with short (less than five methylene functions) chain length thiols, voltammograms have many of the characteristics of that given for azurin immobilised on pyrolytic graphite (Fig. 9(c)). With long chain modifiers (ten or more methylenes), voltammetric responses are characteristic of slow electron transfer rates [50]. In summary, the voltammetry of proteins surface confined to carboxylate-modified carbon electrodes [46] would appear to closely resemble the responses obtained when they are immobilised on short chain length self-assembled thiols.

When electrode processes occur at surfaces with less than a monolayer coverage of facilitator, the nature of the voltammograms is complicated by the fact that uncovered parts of the surface are apparently electroinactive at the reversible potential (see later) and consequently only that part of the surface modified by facilitator gives rise to reversible-type electrochemistry. This voltammetry now occurs, by definition, at an array of electroactive sites, rather than at a fully covered surface (Figs. 12(b) and 13). Under these circumstances, the size and spacing

(coverage) of the electrodes determines the nature of the diffusion problem. Bond [52,53] has employed this model, and, again for a reversible process, ΔE_p values may be in excess of $56/n$ mV for a reversible process. According to this model, the linear diffusion component, usually used to model the voltammetry, is most likely to be approximately correct at very slow scan rates or when the arrays of electroactive sites are closely spaced (Fig. 13(c)). Again, a non-linearity in plotting peak height versus square root of scan rate plots is commonly observed and may be explained with this model. Apparently low diffusion coefficients produced by application of a model assuming a completely electroactive surface will be explicable in terms of a smaller-than-expected electroactive area. In reality, a combination of models a and b, with either reversible or quasi-reversible rates of electron transfer, should be employed to theoretically describe voltammetry at modified gold or functionalised carbon surfaces.

According to the above description, an inherent assumption is that the metalloproteins adsorbed onto bare electrode surfaces act as self-blocking, or insulating, materials at or near to the reversible potential. Thus, we learn from SPM studies that azurin is slowly adsorbed on to a bare gold electrode, and that this time dependent process appears to be associated with the decay of the azurin response from a peak to sigmoidal-shaped curve under the conditions of Fig. 10(a). Analogous surface activity and time dependent voltammetry is observed (Fig. 11(c)) for cytochrome *c* at a bare gold electrode as the effective surface area decreases with time and radial, rather than linear, diffusion increasingly occurs at a partially blocked surface until no voltammetry is observed at the fully blocked surface. Similarly, voltammetry at ex situ modified gold surfaces is time dependent because adsorption of the protein slowly displaces, or sits over, the facilitator and creates a partially-blocked electrode surface. Alternatively, the facilitator may slowly dissolve from the surface to produce patches of bare electrode which provide sites for protein adsorption and concomitant formation of electroinactive surface regions. However, again as shown in Fig. 11(e), a concomitant decrease in current and wave shape occurs in this situation as diffusion changes from being predominantly linear to essentially radial.

The purely surface-confined voltammetry of metalloproteins adsorbed on to carbon electrodes, at submonolayer levels, has been elegantly described by Armstrong et al. [46]. The SPM studies imply that the voltammetry described for surface-confined metalloproteins at freshly prepared and roughened carbon electrodes results from material attached to carboxylate or similar functional surface regions. The usual theory to describe such processes is based on Eq. (3):

$$\begin{aligned} &\mathrm{Az[Cu^{II}]_{surface}} + \mathrm{e^-} \overset{(E^\circ,\ k_s,\ \alpha)_{surface}}{\rightleftharpoons} \mathrm{Az[Cu^{I}]_{surface}} \\ &\mathrm{Cyt\ \ c[Fe^{III}]_{surface}} + \mathrm{e^-} \overset{(E^\circ,\ k_s,\ \alpha)_{surface}}{\rightleftharpoons} \mathrm{Cyt\ \ c[Fe^{II}]_{surface}} \end{aligned} \tag{3}$$

where $(k_s)_{surface}$ now has units of s^{-1} rather than cm s^{-1} (which is the case for the heterogeneous charge transfer rate constant in Eq. (1)).

The conclusions drawn from a comparison of alternative models with conventional models (where electron transfer is assumed to take place at, or very close to,

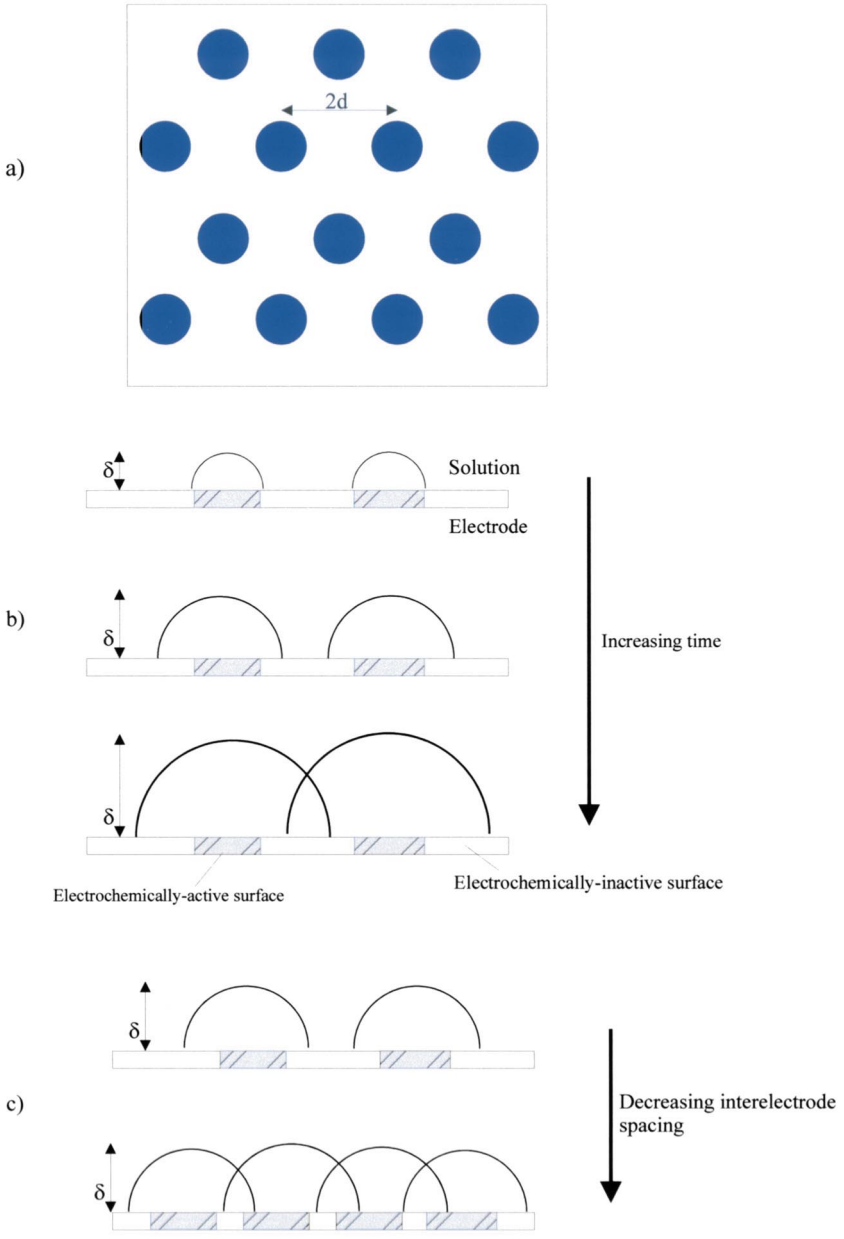

Fig. 13. An idealised representation (a) of the electrode surface as an array of electroactive microelectrode units (of diameter d) and the overlapping of diffusion layers which occurs as time increases (b) and/or interelectrode spacing decreases (c). Such a model is applicable when protein molecules irreversibly adsorb at an electrode and subsequent diffusion of electroactive molecules to the partially blocked surface is predominantly radial in nature. This behaviour is also expected under the conditions of partial ('patchy') coverage of a facilitating adlayer. δ is the diffusion layer thickness.

the electrode surface) are that heterogeneous rates of electron transfer are > 1 cm s^{-1} for diffusion controlled systems and also that the first order electron transfer rates (units s^{-1}) are very fast for diffusionless systems. A plot of first order rate constant against chain length for cytochrome *c* voltammetry at carboxylate-terminated self-assembled monolayers on gold is linear [50]. While a good agreement between values obtained at short chain lengths with those obtained with 4,4′-dithiobipyridine has yet to be reached, there is little doubt that, with such thiol chain lengths, the electron transfer rate is extremely fast. The data obtained with the 'spontaneously modified' carbon electrodes used by Armstrong et al. [46] should be relevant to those observed with short chain lengths in the case of deliberately modified gold surfaces.

5. Summary

The difficulty with interpretation of voltammetric studies of very surface active metalloproteins is that the current values measured represent average values resulting from all events that occur at a particular potential and time domain. Thus, deducing mechanisms and electron transfer rate constants using conventional (often unsubstantiated) voltammetric models, based solely on mass transport of the protein to and from the electrode surface, is fraught with danger. In future, we would hope that the favoured approach in analysis of metalloprotein voltammetry will be to observe and identify the nature of any surface-attached material, the electrode surface topography itself, and the interactions between the two by both scanning probe and spectroscopic methods. A decision can then be made as to what theoretical model should be used in interpretation of voltammetric data. For example, when a protein is adsorbed on to a flat bare electrode, it will appear to be electroinactive at potentials close to that of the reversible value of the native form of the protein, as determined from potentiometric measurements: when it is adsorbed on to a suitably modified electrode surface, it will be able to exchange electrons with the electrode in the appropriate range. Finally, it can be noted that the use of surface or surface-confined models, at chemically modified electrodes, that do not allow for the fact that electron transfer occurs at some distance from the electrode, will almost invariably underestimate the true electron transfer rate constants.

Acknowledgements

The majority of this review was written when A.M.B. was on leave at the Department of Chemistry, University of Oxford, as the 1998 Hinshelwood Lecturer. Grateful acknowledgement is given to Monash University for granting leave and to the University of Oxford for its hospitality during this period. H.A.O.H. and J.J.D. wish to acknowledge Professor Gerard Canters and his group at the Department of Chemistry, Leiden University, Professor F.A. Armstrong and Drs

E.N.K. Wallace and M. Honeychurch (University of Oxford) for useful discussions. H.A.O.H. thanks the BBSRC, EPSRC and Abbott Laboratories for financial support. J.J.D. thanks the Royal Society for support.

References

[1] R.J.P. Williams, Mol. Phys. 68 (1989) 1 and Refs. cited therein.
[2] M.J. Eddowes, H.A.O. Hill, J. Chem. Soc. Chem. Commun. (1977) 771.
[3] P. Yeh, T. Kuwana, Chem. Lett. (1977) 1145.
[4] A.E.G. Cass, G. Davis, G.D. Francis, H.A.O. Hill, I.J. Higgins, E.V. Plotkin, L.D. Scott, A.P.F. Turner, Anal. Chem. 56 (1984) 667.
[5] J. Li, E.K. Wang, Electroanalysis 8 (1996) 107.
[6] J. Wang, Analyst 117 (1992) 1231.
[7] F.A. Armstrong, H.A.O. Hill, N.J. Walton, Acc. Chem. Res. 21 (1988) 407.
[8] F.A. Armstrong, P.A. Cox, H.A.O. Hill, V.J. Lowe, B.N. Oliver, J. Electroanal. Chem. 217 (1987) 331.
[9] G. Binnig, H. Rohrer, Ch. Gerber, E. Weibel, Phys. Rev. Lett. 49 (1982) 57.
[10] G. Binnig, C.F. Quate, C. Gerber, Phys. Rev. Lett. 56 (1986) 930.
[11] G. Binnig, H. Fuchs, Ch. Gerber, H. Rohrer, E. Stoll, E. Tosatti, Europhys. Lett. 1 (1986) 31.
[12] R. Sonnenfeld, P.K. Hansma, Science 232 (1986) 211.
[13] H. Nar, R. Huber, A. Messerschmidt, M. Van der Kamp, G.W. Canters, J. Mol. Biol. 221 (1991) 765.
[14] R. Lontie (Ed.), Copper Proteins and Copper Enzymes, vol. 1, CRC Press, Boca Raton, FL, 1984.
[15] E.T. Adman, Adv. Prot. Chem. 42 (1991) 145.
[16] M. van de Kamp, F.C. Hali, N. Rosato, A.F. Agro, G.W. Canters et al., Biochem. Biophys. Acta 1019 (1990) 283.
[17] T.J. White, N. Arnheim, H.A. Erlich, Trends Genet. 15 (1989) 185.
[18] G.W. Canters, G. Gilardi, FEBS Lett. 325 (1993) 39.
[19] E.P. Friss, J.E.T. Andersen, L.L. Madsen, N. Bonander, P. Moller, J. Ulstrup, Electrochim. Acta 42 (1997) 2889.
[20] J.J. Davis, C.M. Halliwell, H.A.O. Hill, G.W. Canters, M.C. Van Amsterdam, M.P. Verbeet, New J. Chem. (1998) 1119.
[21] P. Tengvall, M. Lestelius, B. Liedberg, I. Lundstrom, Langmuir 8 (1992) 1236.
[22] A. Ihs, B. Liedberg, J. Colloid Interface Sci. 144 (1991) 282.
[23] J.E.T. Andersen, P. Moller, M.V. Pedersen, J. Ulstrup, Surf. Sci. 325 (1995) 193.
[24] J.J. Davis, H.A.O. Hill, unpublished observations, 1997.
[25] J.J. Davis, H.A.O. Hill, unpublished observations, 1999.
[26] J.J. Davis, H.A.O. Hill, A. Kurz, C. Jacob, W. Maret, B.L. Vallee, Phys. Chem. Commun. 1 (1998) http://www.rsc.org/ej/qu/1998/f9806057.
[27] R. Mudhopakay, J.J. Davis, H.A.O. Hill, P. Kyritsis, J. Meyer, J. Inorg. Biochem. 78 (2000) 251.
[28] M.J. Eddowes, H.A.O. Hill, J. Am. Chem. Soc. 101 (1979) 7113.
[29] M.J. Eddowes, H.A.O. Hill, Faraday Discuss. Chem. Soc. 74 (1982) 331.
[30] W.J. Albery, M.J. Eddowes, H.A.O. Hill, A.R. Hillman, J. Am. Chem. Soc. 103 (1981) 3904.
[31] P.M. Allen, H.A.O. Hill, N.J. Walton, J. Electroanal. Chem. 178 (1984) 69.
[32] J.E. Frew, H.A.O. Hill, Eur. J. Biochem. 172 (1988) 261 and Refs. cited therein.
[33] J.J. Davis, H.A.O. Hill, R. Yamada, H. Naohara, K. Uosaki, J. Chem. Soc. Faraday Trans. 94 (1998) 1315.
[34] T. Sawaguchi, F. Mizutani, I. Taniguchi, Langmuir 14 (1998) 3565.
[35] A.S. Lea, A. Pungor, V. Hlady, J.D. Andrade, J.N. Herron, E.W. Voss, Langmuir 8 (1992) 68.
[36] A.J. Bard, L.R. Faulkner, Electrochemical Methods: Fundamentals and Applications, Wiley, New York, 1980.

[37] R.H. Wopschall, I. Shain, Anal. Chem. 39 (1967) 1514.
[38] R.H. Wopschall, I. Shain, Anal. Chem. 39 (1967) 1527.
[39] M.J. Honeychurch, G.A. Rechnitz, J. Phys. Chem. B 101 (1997) 7472.
[40] N.I. Hunt, Ph.D. Thesis, Oxford University, 1994.
[41] M. van der Kamp, M.C. Silvestrini, M. Brunori, J. van Beeumen, F.C. Hali, G.W. Canters, Eur. J. Biochem. 194 (1990) 109.
[42] M. Goldberg, I. Pecht, Biochemistry 15 (1976) 4197.
[43] H.A.O. Hill, N.I. Hunt, A.M. Bond, J. Electroanal. Chem. 436 (1997) 17.
[44] R.W. Henderson, W.R. Rawlinson, Biochemistry 62 (1956) 21.
[45] F.A. Armstrong, P.A. Cox, H.A.O. Hill, B.N. Oliver, A.A. Williams, J. Chem. Soc. Chem. Commun. (1985) 1236.
[46] F.A. Armstrong, H.A. Heering, J. Hirst, Chem. Soc. Rev. 26 (1997) 169.
[47] J.J. Davis, H.A.O. Hill, unpublished observations, 1999.
[48] A.M. Bond, H.A.O. Hill, D.J. Page, I.S.M. Psalti, N.J. Walton, Eur. J. Biochem. 191 (1990) 737.
[49] R.S. Nicholson, Anal. Chem. 37 (1965) 1351.
[50] E.F. Bowden, The Electrochemical Society, Interface (1997) 40 and Refs. cited therein.
[51] A.M. Becka, C.J. Miller, J. Phys. Chem. 96 (1992) 2657.
[52] A.M. Bond, Anal. Proc 29 (1992) 132.
[53] A.M. Bond, Anal. Proc. 30 (1993) 218.
[54] H.A.O. Hill, D.J. Page, N.J. Walton, J. Electroanal. Chem. 217 (1987) 141.
[55] P.D. Barker, K. Di Gleria, H.A.O. Hill, V.J. Lowe, Eur. J. Biochem. 190 (1990) 171.
[56] M. Shibata, K. Nakamura, N. Furuya, M. Watanabe, J. Electroanal. Chem. 314 (1991) 179.
[57] J. Zhao, R.W. Henkens, J. Stonehuerner, J.P. O'Daly, A.L. Crumbliss, J. Electroanal. Chem. 327 (1992) 109.